

Studies on Coherent Synchrotron Radiation at SOLEIL

C. Evain, M.-E. Couprie, M.-A. Tordeux, A. Loulergue, A. Nadji, M. Labat, L. Cassinari,
J.-C. Denard, R. Nagaoka, J.-M. Filhol¹
J. Barros, P. Roy, G. Creff, J.-B. Brubach, L. Manceron¹
A. Zholents²

¹Synchrotron SOLEIL, Saint Aubin, France

²Argonne National Laboratory, Argonne, IL 60439, USA

ESLSW XVIII



Plan

- 1 THz CSR
- 2 Echo on storage rings : femtosecond short-wavelength CSR pulses

Outline

- 1 THz CSR
- 2 Echo on storage rings : femtosecond short-wavelength CSR pulses

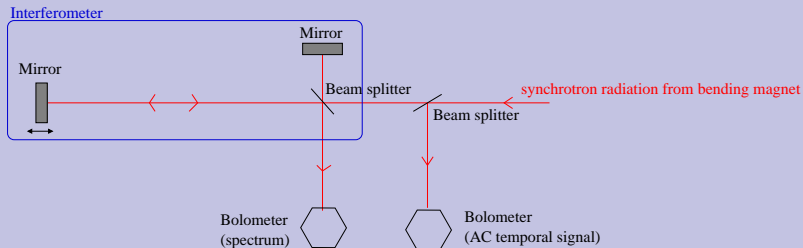
Introduction

- 12/2008 : first observation of THz CSR on the beamline AILES in a low- α mode
- Since 04/2010 : dedicated study machine shifts with the following problematics :
 - THz CSR for user experiments ?
 - Limits of the storage ring in terms of CSR instability ?

Introduction

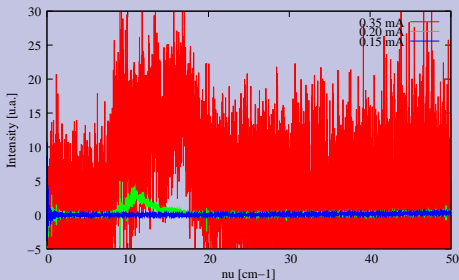
- 12/2008 : first observation of THz CSR on the beamline AILES in a low- α mode
- Since 04/2010 : dedicated study machine shifts with the following problematics :
 - THz CSR for user experiments ?
 - Limits of the storage ring in terms of CSR instability ?

Experimental setup on the beamline AILES (THz and middle-far IR beamline)



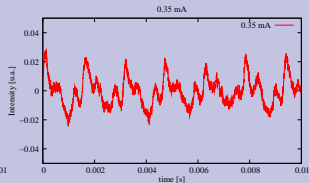
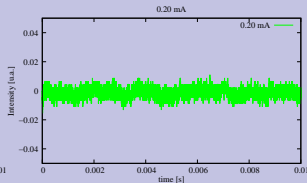
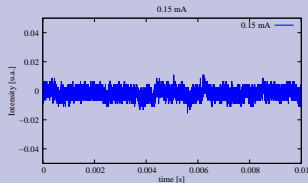
General behavior versus the current (ex : $\alpha/10$)

Associated spectrums



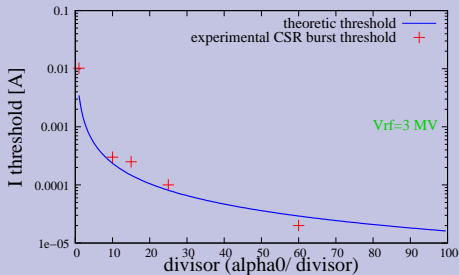
- $\alpha_0 \simeq 4.4 \times 10^{-4}$ (Synchrotron frequency $\simeq 4.5$ kHz at $V_{rf} = 3$ MV)
- Bolometer time resolution < 1 kHz
- Measured RMS e-bunch duration $\simeq 7$ ps (theoretical at zero current $\simeq 5$ ps)
- "Stable" and Bursts THz CSR observed at : BESSY-II, UVSOR-II, ANKA, DIAMOND, ELETTRA, etc.

Temporal signals



CSR burst threshold

Experimental points and analytical threshold



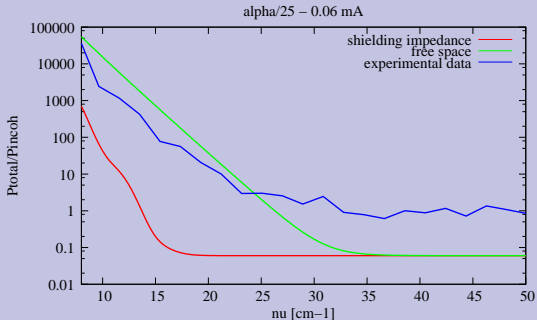
S. Heifest and G. Stupakov analytical threshold [PRST-AB 5 (2002) 064401]

$$kR < 2\Omega^{3/2}$$

with $\Lambda = \frac{IR}{\alpha \Lambda (\sigma_E / E_0)^2 I_A \langle R \rangle}$, $\langle R \rangle = C / 2\pi$, $I_A = 17.5 \text{ kA}$
and $k = 2\pi / \sigma_{z0}$

"Stable" CSR

$$P_{total}/P_{incoherent}$$



- $P_{incoherent}$ @ 400 mA
- P_{total} @ 24 mA (0.06×400 mA)
- Resolution : 0.1 cm^{-1}
- Bolometer time resolution < 1 ms

- Stationary Haissinski solution with **free-space impedance** model and **parallel plate impedance** model [J.B. Murphy et. al., Particule Accelerators 57, 9(1997)] [Y.S Derbenev et. al., TESLA-FEL 95-05 (1995)] [F. Sannibale et al., Phys. Rev. Lett. 93, 094801 (2004)]
- Distance between parallel plates : 2×1.25 cm, bending magnet radius : 5.39 m

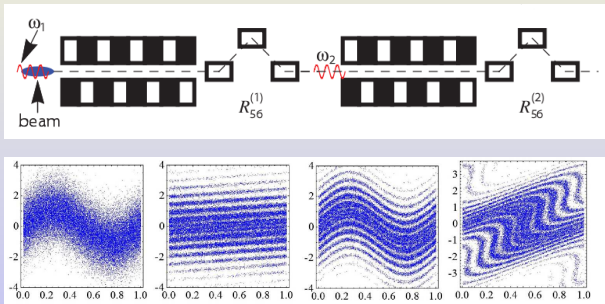
Outline

① THz CSR

② Echo on storage rings : femtosecond short-wavelength CSR pulses

Echo-enable harmonic generation on FEL

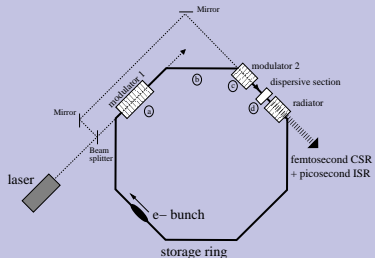
- Principle : G. Stupakov, Phys. Rev. Lett. 102, 074801 (2009)



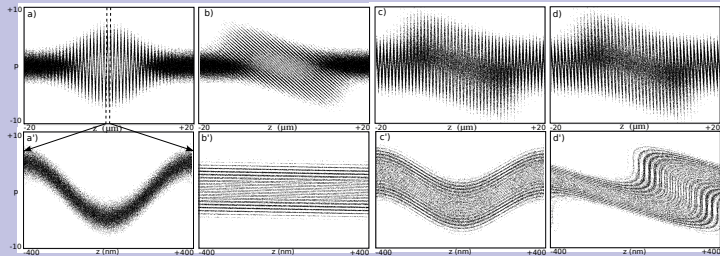
- Proof-of-principle experiment : D. Xiang et. al., Phys. Rev. Lett. 105, 114801 (2010)

Echo on storage ring : principle

Outline

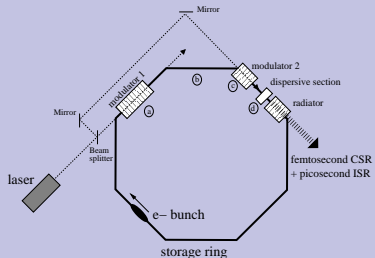


Longitudinal phase space (from 6D tracking simulation including noise from ISR)

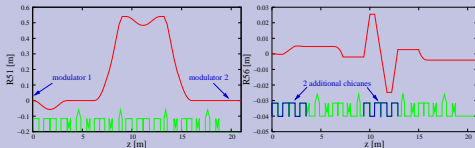


Echo on storage ring : principle

Outline

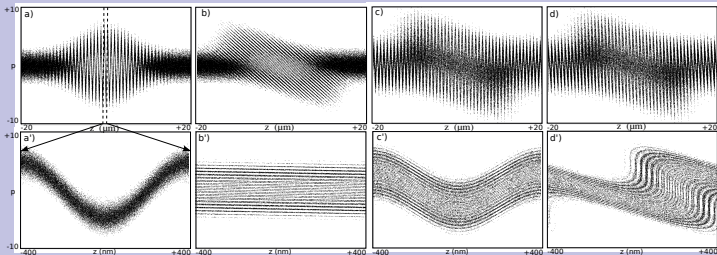


Optics between the two modulators

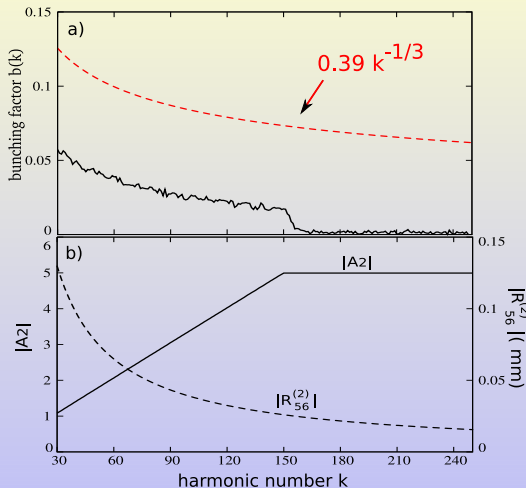


- "zero" transverse dispersion :
⇒ Chasman-Green lattice
- Control of longitudinal dispersion :
⇒ additional chicanes

Longitudinal phase space (from 6D tracking simulation including noise from ISR)



Bunching factor versus wavelength



- $b(k) = \frac{1}{N} | \langle \rho(z) \rangle e^{ikz2\pi/\lambda_L} \rangle |$
- TEMPO beamline undulator ($\lambda_u = 80$ mm, $N_u = 19$, 27.6-0.8 nm, $k \in [29 : 967]$)
- First energy modulation amplitude $A_1 = 5$ (unit of σ_E)
- $R_{56}^{(1)} = 4$ mm

$$b(k) = \left| J_{k+1}[kA_2B_2] J_1[A_1(B_1 - kB_2)] \times e^{-\frac{1}{2}[B_1 - kB_2]^2} \right| \quad [D. Xiang and G. Stupakov, PRSTAB (2009)]$$

$$b(k) \simeq 0.39k^{-1/3} \quad \text{optimized bunching factor} [D. Xiang and G. Stupakov, PRSTAB (2009)]$$

Emitted peak power

- Analytical formula

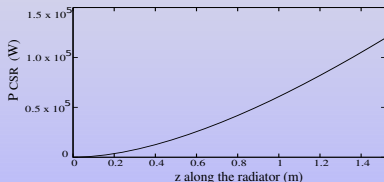
$$P_{CSR} = \pi \alpha \hbar \omega \frac{K^2}{1 + K^2/2} [JJ]^2 \frac{I_{\text{peak}}}{e} n_e b^2 \sqrt{f_2}.$$

- $n_e = \frac{I_{\text{peak}} \lambda_r N_u}{c e}$,
- $f_2 = (\sigma_r \sigma_{r'})^2 / (\sqrt{\sigma_r^2 + \sigma_x^2} \sqrt{\sigma_{r'}^2 + \sigma_{x'}^2} \sqrt{\sigma_r^2 + \sigma_y^2} \sqrt{\sigma_{r'}^2 + \sigma_{y'}^2})$,
- $\sigma_r = \sqrt{2 \lambda_r \lambda_u N_u} / 4\pi$,
- $\sigma_{r'} = \sqrt{\lambda_r / 2 \lambda_u N_u}$.

[Z. Huang and K.-J. Kim, PAC'99]

@ 27.5 nm (800/30 nm) with $b = 5\%$ and $I_{\text{peak}} = 138 \text{ A}$, $P_{CSR} \simeq 187 \text{ kW}$

- With GENESIS :



$$\underline{P'_{CSR} \simeq 120 \text{ kW}}$$

Comparison with slicing power and signal-to-noise ratio

- Slicing power P_{ISR}

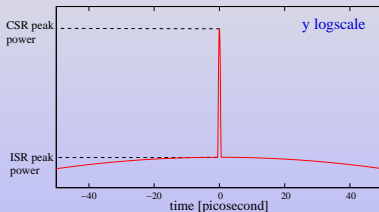
$$P_{ISR} = \dot{N}_{phot} \hbar \omega \times \eta \quad (\eta : \text{percentage of electrons involved in the fs light pulse})$$
$$\dot{N}_{ph}(\omega) = \pi \alpha N_u \frac{\Delta \omega}{\omega} \frac{I_{peak}}{e} \frac{K^2 [JJ]^2}{1 + K^2/2}$$

$P_{ISR} \simeq 0.135 \text{ W}$ at $\lambda_r = 26.7 \text{ nm}$ with $\Delta \omega / \omega = 0.05\%$ and $\eta = 0.1$

$$\underline{P_{CSR}/P_{ISR} \simeq 10^6}$$

- Signal-to-noise-ratio S/N

$$S/N = \frac{P_{CSR} \times \sigma_{L1} \eta c}{P_{ISR} \times \sigma_z}$$
$$= \frac{n_e b^2 \sqrt{F_2} \sigma_{L1} c}{\sigma_z} N_u \frac{\Delta \omega}{\omega}$$
$$\simeq 168$$



Conclusion

THz CSR

- Observation of THz CSR at SOLEIL
- Higher photon flux but lower stability compared to THz ISR and not "smooth" spectrum
⇒ soon conclusion about the utility for user experiments
- Futur project : laser induced THz CSR (with slicing)

EEHG on storage ring

- Femtosecond CSR pulses at short-wavelength
- On the SOLEIL example : until 5 nm and with 6 orders of magnitude power increase compared to slicing at 27 nm
- No direct test possible at SOLEIL without moving presently installed undulators.
- To estimate experimental difficulty : study of the microstructure sensibility to magnetic errors.

Coordinate changes at each step

$$\mathbf{a} \quad \rho = \rho + A_1 \times e^{-\frac{z^2}{2(c\sigma_{L1})^2}} \cos\left(\frac{2\pi}{\lambda_L} z\right) \times e^{-\frac{x^2+y^2}{w_1^2}}$$

$$\mathbf{b} \quad z \simeq z + \rho \times R_{56}^{(1)} \frac{\sigma E}{E_0}$$

$$\mathbf{c} \quad \rho = \rho + A_2 \times e^{-\frac{z^2}{2(c\sigma_{L2})^2}} \cos\left(\frac{2\pi}{\lambda_L} z\right) \times e^{-\frac{x^2+y^2}{w_2^2}}$$

$$\mathbf{d} \quad z \simeq z + \rho \times R_{56}^{(2)} \frac{\sigma E}{E_0}$$

SOLEIL parameters used in our study

Nominal energy E_0 (GeV), energy spread σ_E (MeV)	2.75, 2.79
Bunch dimensions σ_z (mm), σ_x (μm), $\sigma_{x'}$ (μrad)	10.5, 147, 33
Bunch dimensions σ_y (μm), $\sigma_{y'}$ (μrad)	10.0, 4.8
Peak current I_{peak} (A)	134
Radius R (m) and length L (m) of a bending magnet	5.39, 1
Chicane length (m) and field (T)	0.65, 0.7
Modulator 1&2 period length (mm)	150
Modulator 1&2 number of periods	13
Radiator period length λ_u (mm)	80
Radiator number of periods N_u	19
Laser wavelength λ_L (nm)	800
Maximum energy laser pulse (mJ)	5
RMS laser pulse length σ_{L1} (fs), σ_{L2} (fs)	43, 118
